Acta Pharmacologica Sinica (2017) 38: 660–671
 1671-4083/17
www.nature.com/aps

Original Article

Dicer1/miR-29/HMGCR axis contributes to hepatic free cholesterol accumulation in mouse non-alcoholic steatohepatitis

Ming-xia LIU[1, 2], Man GAO[1, 2], Chun-zhu LI[1, 2], Cun-zhi YU[1, 2], Hong YAN[1, 2], Chun PENG[1, 2], Yu LI[1, 2], Cheng-gang LI[1, 2], Ze-long MA[1, 2], Yang ZHAO[1, 2], Meng-fan PU[1, 2], Ling-ling MIAO[1, 2], Xin-ming QI[1, 2, *], Jin REN[1, 2, *]

[1]Center for Drug Safety Evaluation and Research, State Key Laboratory of Drug Research, Shanghai Institute of Materia Medica, Chinese Academy of Sciences, Shanghai 201203, China; [2]Center for Drug Safety Evaluation and Research, State Key Laboratory of Drug Research, Shanghai Institute of Materia Medica, University of Chinese Academy of Sciences, Beijing 100049, China

Abstract

Dicer1 is an enzyme essential for microRNA (miRNA) maturation. The loss of miRNAs resulted from Dicer1 deficiency greatly contributes to the progression of many diseases, including lipid dysregulation, but its role in hepatic accumulation of free cholesterol (FC) that is critical in the development of non-alcoholic steatohepatitis (NASH) remains elusive. In this study, we used the liver-specific Dicer1-knockout mice to identify the miRNAs involved in hepatic FC accumulation. In a widely used dietary NASH model, mice were fed a methionine-choline-deficient (MCD) diet for 3 weeks, which resulted in significant increase in hepatic FC levels as well as decrease of Dicer1 mRNA levels in livers. The liver-specific Dicer1-knockout induced hepatic FC accumulation at 5–6 weeks, accompanied by increased mRNA and protein levels of 3-hydroxy-3-methylglutaryl coenzyme A reductase (HMGCR), a rate-limiting enzyme of cholesterol synthesis in livers. Eleven predicted miRNAs were screened, revealing that miR-29a/b/c significantly suppressed HMGCR expression by targeting the HMGCR mRNA 3'-UTR. Overexpression of miR-29a in SMMC-7721 cells, a steatosis hepatic cell model, significantly decreased HMGCR expression and the FC level. Furthermore, the expression levels of miR-29a were inversely correlated with HMGCR expression levels in the MCD diet mouse model *in vivo* and in 2 steatosis hepatic cell models (SMMC-7721 and HL-7702 cells) *in vitro*. Our results show that Dicer1/miR-29/HMGCR axis contributes to hepatic free cholesterol accumulation in mouse NASH, and miR-29 may serve as an important regulator of hepatic cholesterol homeostasis. Thus, miR-29a could be utilized as a potential therapeutic target for the treatment of non-alcoholic fatty liver disease as well as for other liver diseases associated with FC accumulation.

Keywords: non-alcoholic steatohepatitis; cholesterol accumulation; Dicer1; HMGCR; microRNA-29; MCD diet-treated mice

Acta Pharmacologica Sinica (2017) 38: 660–671; doi: 10.1038/aps.2016.158; published online 23 Jan 2017

Introduction

Currently, non-alcoholic fatty liver disease (NAFLD) is recognized as the most common liver disease worldwide, affecting 25%–30% of the general population[1], and 10%–15% of NAFLD patients progress to irreversible non-alcoholic steatohepatitis (NASH)[2]. Currently, NAFLD has become a global challenge to health.

Ectopic hepatic lipid accumulation, especially free cholesterol (FC), has been demonstrated to promote the progression of NAFLD[3–5], especially NASH. FC accumulation is one of the hallmarks of NAFLD, which promotes steatohepatitis and liver fibrosis and correlates with the histological severity of the disease[3, 6]. Abundant FC in the liver causes liver injury that induces inflammation and fibrogenesis[7], mediated by the increased production of reactive oxygen species (ROS) resulting in mitochondrial dysfunction, and by triggering the unfolded protein response (UPR) in the endoplasmic reticulum (ER), which causes ER stress and apoptosis[8]. Cholesterol accumulation may be attributed to increased *de novo* synthesis[9], increased uptake from lipoproteins[10], decreased conversion to bile acids[11] or decreased cholesterol excretion in the bile[3]. However, the molecular mechanism triggering these abnormalities and the relative contribution of these pathways to cholesterol accumulation in NAFLD remain to be elucidated.

Dicer, an RNase III endonuclease, is required for the maturation of microRNAs (miRNAs)[12–14]. A previous study showed that Dicer is involved in the maintenance of normal

*To whom correspondence should be addressed.
E-mail jren@cdser.simm.ac.cn (Jin REN);
qixinming@icloud.com (Xin-ming QI)
Received 2016-10-11 Accepted 2016-11-22

cholesterol metabolism, and the disruption of Dicer1 in mouse livers caused a remarkable elevation of cholesterol ester (CE) and a mild increase of FC[15], although the mechanisms underlying this phenomenon are not fully understood. Crucially, the disruption of the Dicer1 gene results in the loss of mature miRNAs[15–17]. Recent studies have suggested that miRNAs are highly associated with the maintenance of hepatic cholesterol homeostasis by regulating target gene expression post-transcriptionally[18]. The miR-34a levels are elevated in the livers of humans with NAFLD/NASH[19, 20], which enhances 3-hydroxy-3-methylglutaryl coenzyme A reductase (HMGCR) dephosphorylation and causes cholesterol accumulation[3] by targeting the hepatic NAD-dependent deacetylase Sirtuin 1[21]. miR-33a/b represses key genes involved in cellular cholesterol export and high-density lipoprotein (HDL) metabolism, such as the adenosine triphosphate binding cassette (ABC) transporters, ABCA1 and ABCG1, and the endolysosomal transport protein Neimann Pick C1 (NPC1)[22, 23]. Although miR-33 antagonism remarkably increases HDL and lowers very low-density lipoprotein (VLDL), one recent study reported that long-term inhibition of miR-33 may increase CEs and triglycerides (TGs), leading to hepatic steatosis in mice fed a high-fat diet[24]. Hepatic miR-122 is decreased in the livers of NASH patients, while it is increased in the blood[19, 25, 26]. The silencing of miR-122 caused an accumulation of both cholesterol and TGs in mouse livers[27, 28]. However, the HMGCR level was significantly decreased after miR-122 silencing[28], which is not consistent with the increased HMGCR expression in NAFLD patients[3]. The direct targets of miR-122 are still unknown. Taken together, these lines of evidence provide a strong indication that other microRNAs may play critical roles in the process of hepatic FC accumulation in NAFLD.

To elucidate the role of Dicer and miRNAs in liver cholesterol homeostasis, we used a liver-specific Dicer1-knockout (KO) mouse model[15, 29] to address the mechanisms of Dicer1-deficient-induced hepatic cholesterol accumulation *in vivo*. The methionine-choline deficient (MCD) diet mouse model is a frequently used nutritional model of NASH. The MCD diet model has the advantage of being more efficient and reproducible for inducing severe liver damage and progressive fibrosis[30]. We used this model to explore the Dicer1 expression in NASH and to perform correlation analysis of miR-29a and HMGCR. Our results showed that miR-29s directly regulates HMGCR expression and that a novel Dicer1/miR29s/HMGCR regulatory circuit contributes to FC accumulation in NAFLD.

Materials and methods

Animals

The liver-specific Dicer1-KO C57BL/6 mouse strain (Albumin-Cre; Dicer1$^{loxP/loxP}$ mice) was a kind gift from Prof Yi-zheng WANG (Beijing Institute of Basic Medical Sciences, China). All animal treatments were approved by the Institutional Animal Care and Use Committee of the Shanghai Institute of Materia Medica (Shanghai, China). Animals were maintained at 23±1 °C with a 12 h on and 12 h off light cycle. Regular laboratory chow and filtered tap water were allowed *ad libitum*. The male liver-specific Dicer1-KO C57BL/6 mice (n=6–7 for each group) and their control littermates (n=5–6 for each group) were sacrificed at different ages (3 weeks, 4 weeks, 5 weeks and 6 weeks) after an overnight fast. Blood samples were collected immediately and serum was obtained by centrifugation at 4000 r/min for 10 min at 4 °C. The liver tissues were removed and weighed. A portion of fresh tissue was fixed in 10% buffered formalin; the remaining tissues were immediately frozen in liquid nitrogen and then stored at -80 °C until use.

Male C57BL/6 mice (8 weeks old) were fed a methionine/choline supplemented (MCS) control diet or an MCD diet for 3 weeks (n=6 for each group). The MCD diet (TP 3006) and MCS diet (TP 3006S) were both purchased from TROPHIC Animal Feed High-tech Co, Ltd (Nantong, Jiangsu, China). Samples were collected as described above.

Cell culture, transfection and treatment

The human cell lines HepG2, SMMC-7721 and HL-7702 were obtained from the Shanghai Institutes for Biological Sciences, Chinese Academy of Sciences. HepG2 cells were cultured in high-glucose Dulbecco's modified Eagle's medium (DMEM) (HyClone, Logan, UT, USA) supplemented with 10% fetal bovine serum (FBS) (Gibco, Carlsbad, CA, USA) and 1% antibiotic-antimycotic (Gibco). SMMC-7721 cells and HL-7702 cells were cultured in RPMI-1640 medium (Gibco) supplemented with 10% FBS (Gibco) and 1% antibiotic-antimycotic (Gibco). Cells were cultured at 37 °C in 5% CO_2. Lipofectamine 2000 (Invitrogen, Carlsbad, CA, USA) was used for transfection. At least three replicates of each transfection were performed.

SMMC-7721 and HL-7702 cells were incubated in medium containing 10 μg/mL cholesterol (Sigma, St Louis, MO, USA) and 1 μg/mL 25-hydroxycholesterol (Sigma)[31] for 24 h, 48 h or 72 h, and the cell samples were then harvested for further analysis. SMMC-7721 and HL-7702 cells were also incubated in 50% FBS[32] for 24 h, 48 h or 72 h, and the cell samples were then harvested for further analysis. At least three replicates of each experiment were performed.

Serological analysis and liver lipid analysis

Serum alanine aminotransferase (ALT), aspartate transaminase (AST), total cholesterol (TC), HDL cholesterol (HDL-C) and LDL cholesterol (LDL-C) were determined using an automatic HITACHI Clinical Analyzer Model 7080 (Hitachi High-Technologies Corporation, Tokyo, Japan).

Liver TC and FC levels were assayed using enzymatic reagent kits (E1015, E1016, Applygen Technologies Inc, Beijing, China) according to the manufacturer's instructions.

Histologic analysis

Liver tissue specimens were fixed in 10% neutral buffered formalin, and then paraffin-embedded sections were subjected to standard hematoxylin-eosin (H&E) staining.

To measure lipid droplet accumulation in the liver, the tissue was embedded in an optimal cutting temperature (OCT) compound (Tissue-Tek, Torrance, CA, USA). Frozen liver

sections (10 μm) were prepared using a cryostat. After washing with 60% isopropanol, the frozen sections were stained with Oil red O (Sigma, St Louis, USA) solution (in 60% isopropanol) for 5 min, washed repeatedly with PBS, counterstained with hematoxylin for 30 s, and analyzed by light microscopy.

Quantitative real-time reverse transcription-polymerase chain reaction (qRT-PCR)

Total RNA was isolated from the mouse liver tissues or HepG2 or SMMC-7721 cells by UNIQ-10/Trizol total RNA extraction kit (Sangon, Shanghai, China) and reverse-transcribed to cDNA with PrimeScript RT Reagent Kit (Takara, Otus, Shiga, Japan). The primer sets used are listed in Table 1. Quantitative real-time RT-PCR (qRT-PCR) analysis was performed using SYBR® Premix Ex Taq™ (Takara, Otus, Shiga, Japan).

Table 1. Sequence of primers for qRT-PCR analysis. F, forward; R, reverse; m, mouse; h, human.

Gene	Sequence (5′–3′)
m-Dicer1-F	GGTCCTTTCTTTGGACTGCCA
m-Dicer1-R	GCGATGAACGTCTTCCCTGA
m-HMGCR-F	AGCTTGCCCGAATTGTATGTG
m-HMGCR-R	TCTGTTGTGAACCATGTGACTTC
m-ACAT2-F	CCCGTGGTCATCGTCTCAG
m-ACAT2-R	GGACAGGGCACCATTGAAGG
m-CES3-F	TGGTATTTGGTGTCCCATCA
m-CES3-R	GCTTGGGCGATACTCAAACT
m-ABCG5-F	AGGGCCTCACATCAACAGAG
m-ABCG5-R	GCTGACGCTGTAGGACACAT
m-ABCG8-F	CTGTGGAATGGGACTGTACTTC
m-ABCG8-R	GTTGGACTGACCACTGTAGGT
m-LDLR-F	TCAGACGAACAAGGCTGTCC
m-LDLR-R	CCATCTAGGCAATCTCGGTCTC
m-SR-B1-F	AAACAGGGAAGATCGAGCCAG
m-SR-B1-R	GGTCTGACCAAGCTATCAGGTT
m-CYP7A1-F	GGGATTGCTGTGGTAGTGAGC
m-CYP7A1-R	GGTATGGAATCAACCCGTTGTC
m-CYP27A1-F	CTATGTGCTGCACTTGCCC
m-CYP27A1-R	GGGCACTAGCCAGATTCACA
m-GAPDH-F	GGCTACACTGAGGACCAGGTT
m-GAPDH-R	TGCTGTAGCCGTATTCATTGTC
h-HMGCR-F	ACAATAAGATCTGTGGTTGGAATTATGA
h-HMGCR-R	CCTAAAATTGCCATTCCACGAGCAATAT
h-GAPDH-F	GGTGGTCTCCTCTGACTTCAACA
h-GAPDH-R	GTTGCTGTAGCCAAATTCGTTGT

For detecting mature miR-29a, miRNAs were isolated from cells or liver tissues using the mirVana miRNA Isolation Kit (Ambion, Austin, TX, USA) according to the manufacturer's instructions. Reverse transcription and detection of miR-29a were carried out using NCode VILO miRNA cDNA Synthesis Kit and EXPRESS SYBR GreenER miRNA qRT-PCR Kit, respectively (Invitrogen, Carlsbad, CA, USA) according to the manufacturer's instructions. RNU6-2 was used as an internal loading control.

Western blotting assay

Mouse liver tissues were lysed in RIPA lysis buffer (Sangon, Shanghai, China) with phenylmethanesulfonyl fluoride (PMSF). Proteins (12 μg) were separated on 10% SDS-polyacrylamide gels (SDS-PAGE) and transferred electrophoretically onto a polyvinylidene difluoride (PVDF) membrane (Millipore, Billerica, MA, USA). After blocking in 5% nonfat milk in TBST (Tris-buffered saline containing 0.1% Tween-20, pH 7.6) at room temperature for 2 h, the membranes were incubated at 4 °C overnight with the following primary antibodies: anti-GAPDH (1:10000, 2118S, Cell Signaling Technology, Danvers, USA), anti-CES3 (1:100, af5985, R&D Systems, Minneapolis, USA), anti-HMGCR (1:200, sc-33827, Santa Cruz Biotechnologies, CA, USA), anti-ABCG5 (1:100, sc-25796), anti-ABCG8 (1:100, sc-30111), anti-ACAT2 (1:1000, sc-30279), anti-CYP7A1 (1:50, sc-25536), anti-LDLR (1:150, ab30532, Abcam, Cambridge, UK), anti-CYP27A1 (1:1000, ab126785) and anti-SR-B1 (1:1000, ab52629). The membranes were then incubated with HRP-labeled secondary antibodies at room temperature for 1 h, and visualized using an enhanced chemiluminescence detection system (Millipore, Billerica, MA, USA). GAPDH was selected as the internal control.

SMMC-7721, HL-7702 or HepG2 cell samples were also lysed in RIPA lysis buffer with PMSF, and the polyclonal antibody against HMGCR (1:1000, ABS229, Millipore) was used for detection.

Luciferase reporter assay

The 3′UTR of human HMGCR (NM_000859, 1759 bp, GenBank) was amplified via PCR using the genomic DNA of 293 cells. The forward primer used was: 5′-TAGGCGATCGCTCGAGATAGCCCGACAGTTCTGAAC-3′, and the reverse primer was: 5′-TTGCGGCCAGCGGCCGCTTGGTATTAACTTCCTTTTC-3′. Then, the PCR fragment was inserted into the psiCHECK-2 vector (Promega, Madison, WI, USA) with the In-fusion Advantage PCR Cloning Kit (Clontech, Mountain View, CA, USA).

HepG2 cells were co-transfected with the HMGCR 3′-UTR and miR-29 mimics or their seed region mutants (GenePharma, Shanghai, China). After 72 h, the luciferase activity was analyzed using the Dual-Luciferase Reporter Assay System (Promega) according to the manufacturer's protocol. Three independent co-transfection experiments were carried out.

Cellular free cholesterol measurement by GC-MS

The SMMC-7721 cells were transfected with miR-29a mimics and cell samples were harvested after 72 and 96 h. Cellular FC was analyzed by GC-MS according to published protocols[33]. Briefly, the cell samples scraped from each well of a 6-well plate were divided into two parts. One part was used to determine the protein concentration by the Pierce™ BCA Protein Assay Kit (Thermo Fisher, Waltham, MA, USA). The other part was resuspended in 400 μL water and 100 μL of 1 μg/mL deuterated internal cholesterol standard ([2H 2,2,3,4,4]choles-

terol) in isopropanol. The cell suspension was then added to two milliliters of hexane: isopropanol (3:2) and 20 μL of acetic acid. Cholesterol and its derivatives present in the organic phase were collected after vortexing and centrifugation at 2000 rpm for 3 min. The aqueous phase was re-extracted in 1 mL hexane followed by vortexing and centrifugation. The hexane layer was collected and combined with the previous organic phase and then was dried under nitrogen for free cholesterol quantification. Then, 50 μL HTP (HMDS+TMCS+Pyridine) was added to the dried cholesterol preparations and trimethylsilyl (TMS) derivatives were formed in a 1 h incubation at 90 °C. Then, samples were analyzed by GC-MS using a Shimadzu GC-2010 Plus GC-MS instrument (Shimadzu Europa GmbH, Duisberg, Germany). The reagents used in this part of the study were purchased from Sigma. Each assay was performed at least three times.

Statistical analysis

Statistical significance in this study was assessed by Student's *t*-test or one-way ANOVA followed by Tukey's *post hoc* test. Correlation coefficients (*r*) were determined by Pearson's correlation test. *P*-values were considered significant at <0.05.

Results

Dicer1 mRNA expression is reduced in MCD diet mouse model

The MCD diet mouse model is a widely used model to study NAFLD currently. We detected whether Dicer1 expression was associated with NAFLD by using the MCD diet mouse model. The body weights were decreased, and the levels of serum AST and ALT were increased in mice fed the MCD diet for 3 weeks compared with mice fed the MCS diet (Figure S1). In MCD-fed mice, steatosis and inflammatory infiltration were marked in histopathological liver specimens (Figure 1A). The liver FC levels were also significantly increased in mice fed the MCD diet compared with mice fed MCS diet (Figure 1B). Dicer1 mRNA expression revealed significant downregulation in the MCD-fed mice (Figure 1C). Moreover, the Dicer1 level was inversely associated with hepatic FC level (P=0.0068, Figure 1D), suggesting that Dicer1 might be involved in the progression of NAFLD.

Dicer1-deficient livers exhibit increased cholesterol accumulation

To gain a better insight of the underlying regulatory mechanism of Dicer1 and miRNAs in NAFLD, we investigated this further by utilizing a Dicer1-knockout mouse strain.

To test Dicer1 knockout efficiency, we examined the mRNA expression of Dicer1 in the liver. As expected, we observed a loss of Dicer1 mRNA in livers from hepatocyte-specific Dicer1-KO mice at 3, 4, 5 and 6 weeks after birth (Figure 2A). Serum analyses of ALT (Figure 2B) and AST (Figure 2C) revealed significant increases that would indicate liver dysfunction in Dicer1-deficient mouse.

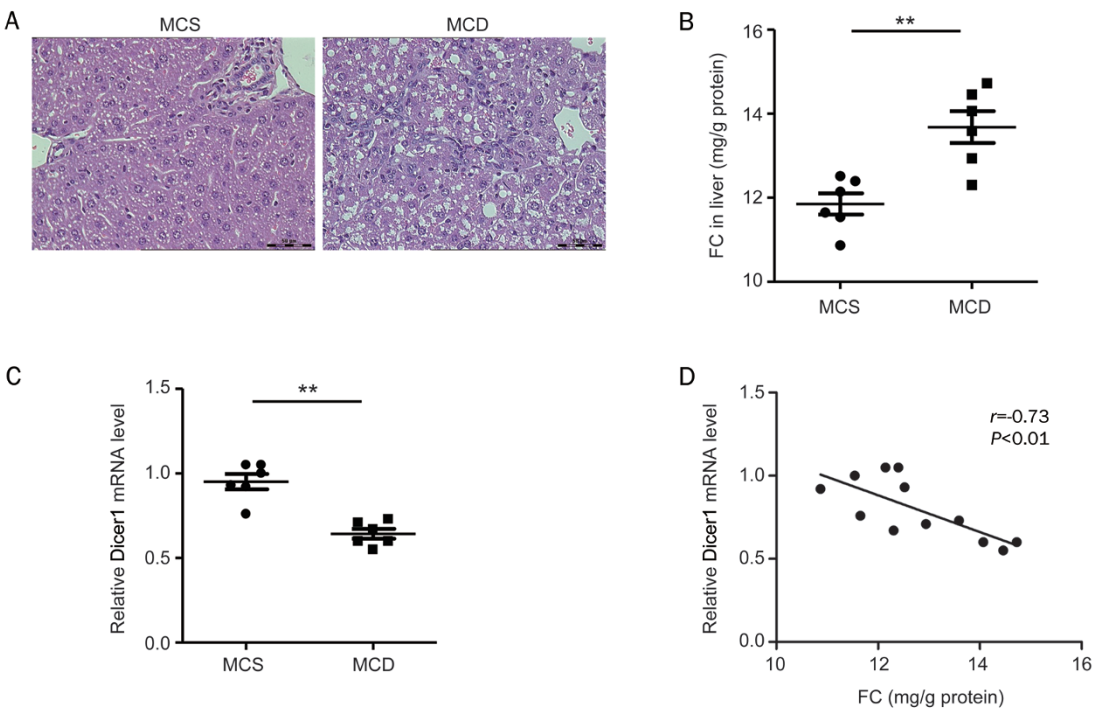

Figure 1. Hepatic Dicer1 mRNA is reduced in MCD-fed mice compared with MCS-fed mice. C57BL/6 mice were fed either methionine-choline supplemented (MCS) control diet or methionine-choline deficient (MCD) diet for 3 weeks (n=6 for each group). Hematoxylin-eosin (H&E) staining of liver sections (A). Free cholesterol (FC) (B) in livers was assayed using enzymatic reagent kits. Dicer1 mRNA level (C) was determined by qRT-PCR, and was associated with the hepatic FC level (D). Correlation between Dicer1 mRNA level and FC level (D) was determined by Pearson's correlation test. *r*, Pearson's correlation coefficient. Mean±SEM. $^{**}P$<0.01.

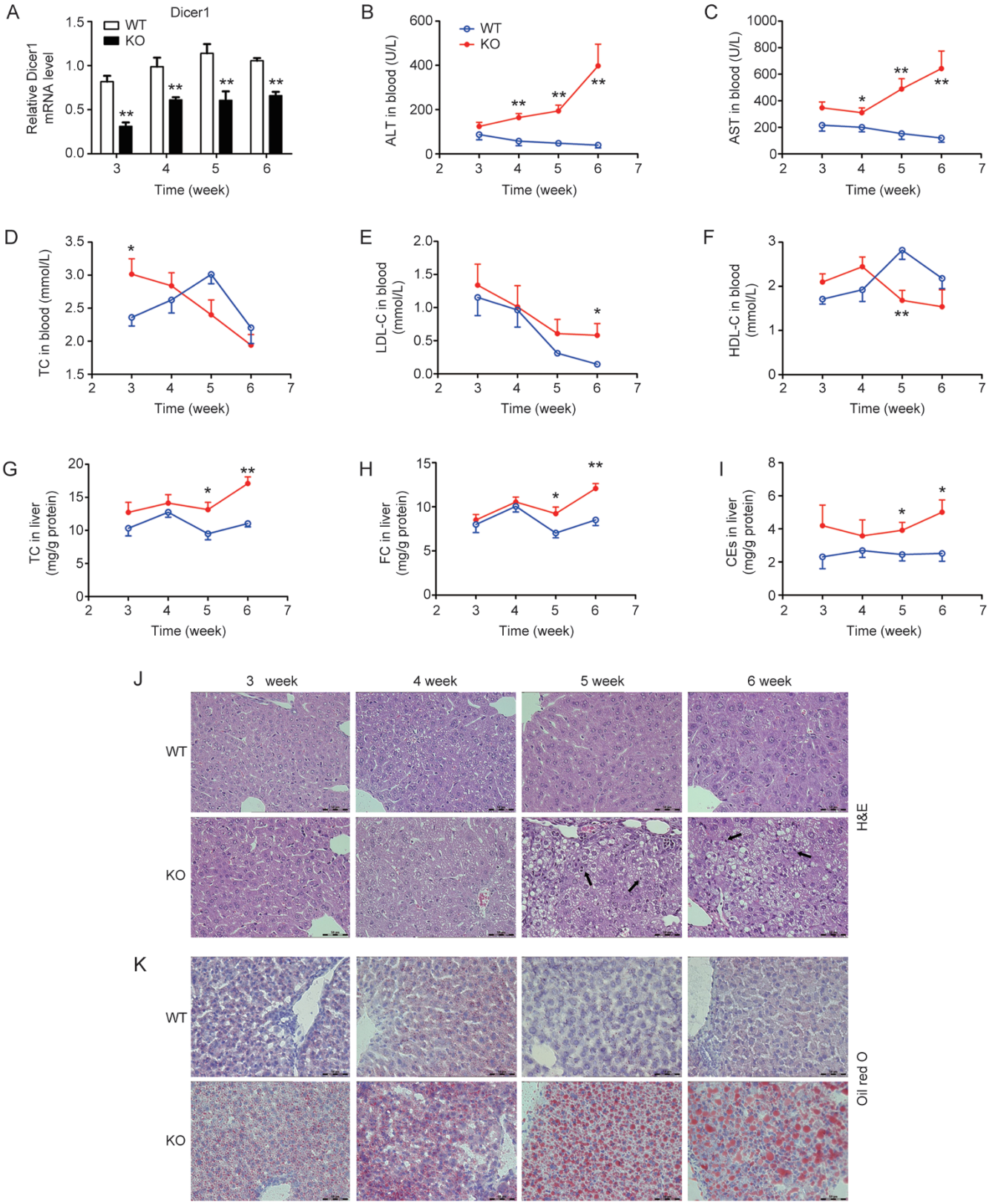

Figure 2. Dicer1-deficient livers exhibit increased cholesterol accumulation. Blood and liver samples of Dicer1-knockout mice (KO) and their control littermates (WT) from 3 to 6 weeks after birth were collected. (A) Dicer1 mRNA levels were reduced in KO mice compared to WT. (B) ALT, (C) AST, (D) total cholesterol (TC), (E) LDL cholesterol (LDL-C) and (F) HDL cholesterol (HDL-C) in blood. (G) Total cholesterol (TC), (H) free cholesterol (FC) and (I) cholesterol esters (CEs) in livers. (J) Hematoxylin-eosin (H&E) staining of liver sections. Arrows, infiltration of inflammatory cells. (K) Oil red O staining of liver sections. Scale bars, 50 μm. All of the values are expressed as the mean±SEM. n=5–7. $^{*}P$<0.05, $^{**}P$<0.01.

Serum TC levels exhibited a significant increase in 3-week-old Dicer1-KO mice (Figure 2D). Serum LDL-C (Figure 2E) descending in WT mice seemed to be delayed by Dicer1-KO, while serum HDL-C levels (Figure 2F) decreased in 5- to 6-week-old Dicer1-KO mice. A detailed analysis of the lipid composition revealed a notable elevation of TC levels, FC levels and CEs levels in 5- and 6-week-old Dicer1-KO mouse livers (Figure 2G, 2H and 2I), representing prominent cholesterol accumulation.

Histologic analysis by H&E staining (Figure 2J) displayed that Dicer1-deficient livers exhibited numerous small cytoplasmic vacuoles and mild hepatitis. Mutant tissue exhibited larger vacuoles and infiltration of inflammatory cells, particularly in the 5- and 6-week-old Dicer1-KO mouse livers. Six-week-old Dicer1-KO mouse livers displayed round nodules consisting of enlarged but otherwise normal hepatocytes, in agreement with a previous study[3]. Oil-Red O staining (Figure 2K) of frozen liver sections revealed numerous lipid droplets in the Dicer1-deficient livers, especially in 5- and 6-week-old mice.

In effect, our results showed that Dicer1-KO mouse livers display similar characteristics to the livers of NAFLD patients and that these animals can be potentially used as a good model for studying the signaling pathways involved in the development of this disease.

Expression of genes regulating cholesterol metabolism is altered in Dicer1-deficient livers

To explore the reasons underlying cholesterol accumulation in the Dicer1-deficient hepatocytes, we examined the mRNA and protein expression of key genes known to be involved in cholesterol metabolism, including cholesterol synthesis, esterification, uptake, utilization and transport.

HMGCR is the rate-limiting enzyme for cholesterol synthesis[34]. HMGCR mRNA was increased in the livers of 4- and 5-week-old Dicer1-deficient mice (Figure 3A), and the protein levels were increased at 5 and 6 weeks (Figure 3B and 3C). HMGCR protein expression was correlated with FC in livers at 5 weeks (P=0.014) (Figure 3D).

Newly synthesized cholesterol is esterified and de-esterified by acyl-CoA cholesterol: cholesteryl transferase 2 (ACAT2)[35] and cholesteryl ester hydrolase (CEH), respectively. The ACAT2 mRNA expression was increased in the 4- and 5-week-old Dicer1-KO mouse livers, while the protein levels were only increased in 5-week-old livers (Supplementary Figure S2A, S2B and S2E). Hepatic carboxylesterase 3 (CES3), the mouse homolog of human CEH, modulates the hydrolysis of lipoprotein-delivered CEs[36, 37]. The CES3 mRNA expression was downregulated significantly, while the protein levels only showed a decrease at 3 weeks (Supplementary Figure S2C,

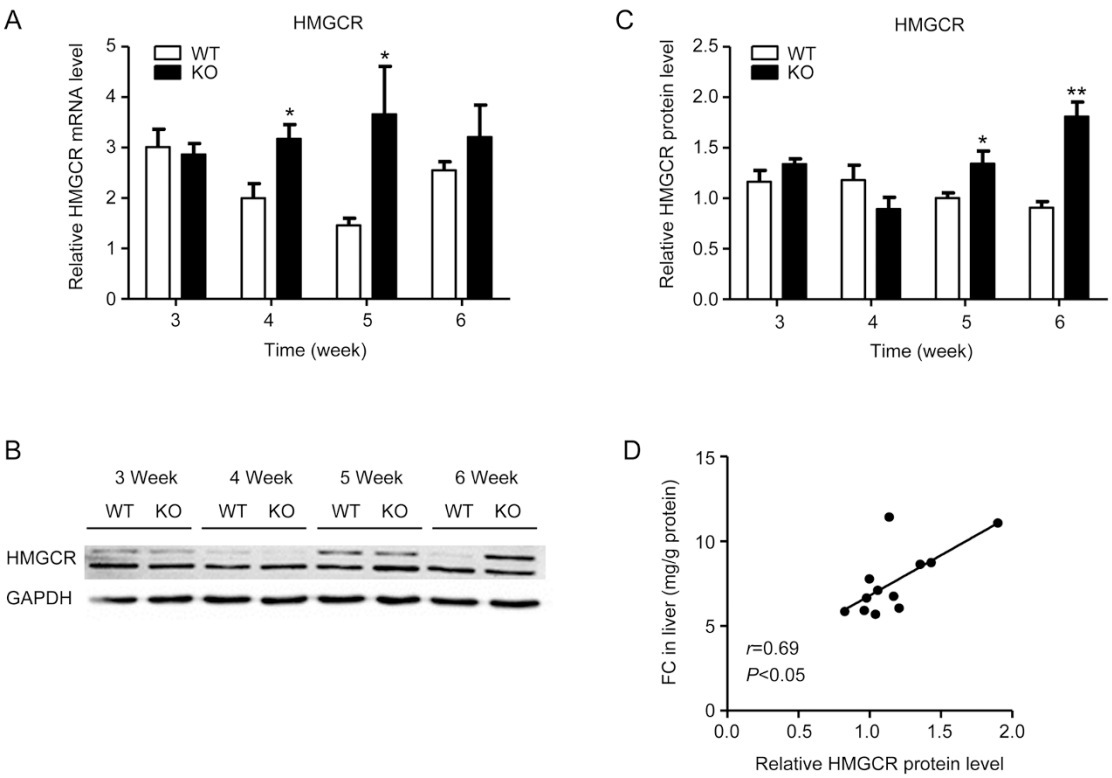

Figure 3. The mRNA and protein expression of HMGCR was upregulated in Dicer1-deficient livers. HMGCR mRNA (A) levels in KO and WT mouse livers were detected by qRT-PCR (n=5–7 for each group). Protein levels of HMGCR (B) were detected by Western blot and quantified with ImageQuant Software (C). HMGCR protein expression level was correlated with FC in 5-week-old mouse livers (P=0.014) (D). Protein levels of HMGCR were normalized to those of GAPDH. Correlation between HMGCR protein level and FC level (D) was determined by Pearson's correlation test. r, Pearson's correlation coefficient. All of the values are expressed as the mean±SEM. $^{*}P$<0.05, $^{**}P$<0.01.

S2D and S2E).

The cholesterol 7a hydroxylase 1 (CYP7A1) and cholesterol 27a hydroxylase 1 (CYP27A1) proteins are both involved in the catabolism of cholesterol to bile acids[11]. The CYP7A1 mRNA was almost not altered (Supplementary Figure S2F). However, the protein levels of CYP7A1 were decreased in 3 and 4-week-old Dicer1-KO mouse livers, and then increased dramatically in 5 and 6-week-old Dicer1-KO mouse livers (Supplementary Figure S2G and S2J). Although the CYP27A1 mRNA levels decreased markedly in all four groups, the protein levels were only decreased in 5- and 6-week-old Dicer1-KO mouse livers (Supplementary Figure S2H, S2I and S2J).

The uptake of LDL-C from the blood into hepatocytes is mediated via the LDL receptor (LDLR)[38]. The mRNA and protein levels of LDLR were nearly unchanged, except when protein levels significantly increased in 3-week-old Dicer1-KO mouse livers (Supplementary Figure S3A, S3B and S3E). Scavenger receptor class B type 1 (SR-B1) in hepatocytes mediates the selective uptake of cholesteryl esters from HDL[39]. The mRNA levels of SR-B1 were decreased in 5- and 6-week-old Dicer1-KO mouse livers, but the protein levels showed an increasing trend only in 6-week-old Dicer1-KO mouse livers (Supplementary Figure S3C, S3D and S3E).

Hepatic cholesterol excretion through bile is regulated via the adenosine triphosphate binding cassette subfamily G member 5/8 (ABCG5/8)[40]. Both the mRNA and protein levels of ABCG5 did not change (Supplementary Figure S3F, S3G and S3J). The ABCG8 mRNA levels were decreased significantly in 6-week-old Dicer1-KO mouse livers, while ABCG8 protein levels were still unchanged (Supplementary Figure S3H, S3I and S3J).

Briefly, our results showed that cholesterol accumulating in the Dicer1-KO mouse livers could be due to alterations of HMGCR expression, which is involved in the biosynthesis of cholesterol but not in other pathways. We should focus on HMGCR in further studies to explore the relationship between HMGCR and Dicer1 deficiency.

miR-29 family downregulates HMGCR expression

The increase of both the mRNA and protein expression of HMGCR in Dicer1-deficient animals suggested that this might be due to the loss of miRNAs involved in the regulation of HMGCR. Based on sequence analysis and using the bioinformatics tool, TargetScan (http://www.targetscan.org/), we predicted 11 miRNAs that may potentially regulate the expression of HMGCR. Further analysis of the candidate miRNAs showed that miR-29a, miR-29b and miR-29c could inhibit HMGCR mRNA and protein levels in SMMC-7721, HepG2 and HL-7702 cells (Figure 4A–4F). Due to the dominant role of miR-29a in the miR-29 family in mouse and human liver[41], we focused on miR-29a as the miR-29 family member representative for the repression of HMGCR in the liver. As expected, transfection with the miR-29a expressing constructs significantly reduced the FC levels in SMMC-7721 cells after 72 h and 96 h (Figure 4G).

Luciferase reporter assays showed that miR-29s decreased HMGCR 3′-UTR luciferase activity. This inhibitory effect was lost when mutations in the seed regions of miR-29s were introduced. These results suggest that miR-29a, miR-29b and miR-29c can directly bind to the HMGCR 3′-UTR region through their seed region to downregulate HMGCR expression (Figure 4H–4K).

miR-29a levels inversely correlated with HMGCR levels *in vitro*

To further elucidate the role of miR-29a in cholesterol homeostasis, we addressed whether miR-29a expression was regulated in response to the levels of cholesterol *in vitro*. SMMC-7721 cells and HL-7702 cells were treated with or without cholesterol and 25-hydroxycholesterol to establish an *in vitro* model of cholesterol accumulation, and the HMGCR and miR-29a expression profiles were determined. When the SMMC-7721 cells were treated with cholesterol and 25-hydroxycholesterol, the miR-29a expression was induced 1.65-fold (Figure 5A), while the HMGCR mRNA and protein expression were reduced by nearly 30% and 35%, respectively, at 48 h (Figure 5B and 5C) compared to control cells. In HL-7702 cells, miR-29a expression was induced 2-fold (Figure 5D), while HMGCR protein expression was reduced by nearly 65% at 72 h (Figure 5F) and the HMGCR mRNA level was also decreased (Figure 5E) compared to control cells. Similarly, in the other set of experiments, when SMMC-7721 and HL-7702 cells were incubated in 50% FBS, miR-29a levels were also upregulated and the expression levels of the HMGCR mRNA and protein were markedly reduced at 24 h, 48 h and 72 h compared to those in 10% FBS (Figure 5G–5L).

miR-29a levels inversely correlated with HMGCR levels *in vivo*

Furthermore, the *in vivo* effect of miR-29a was explored in the MCD diet mouse model. The miR-29a level was reduced significantly (Figure 6A), showing an inverse correlation with the HMGCR mRNA that was upregulated (P=0.04) (Figure 6B and 6C). Interestingly, the cellular FC level in mouse livers was inversely correlated with miR-29a (Figure 6D) and was positively correlated with the HMGCR level (Figure 6E).

Discussion

The liver plays a central role in the regulation of cholesterol metabolism. Abnormal intrahepatic cholesterol loading can promote hepatic steatosis and inflammation[42]. Emerging evidence suggests that hepatic FC is a major lipotoxic molecule critical in the development of experimental and human NAFLD. Therefore, it is essential to understand the molecular mechanisms of cholesterol accumulation involved in the progression of NAFLD[3, 43].

In our study, FC accumulation in the Dicer1-KO mouse liver was most likely due to its increased synthesis, resulting from the increased expression levels of HMGCR. Cholesterol uptake and excretion seemed not to contribute to cholesterol accumulation in this mouse model, as the LDLR, SR-B1, ABCG5 and ABCG8 protein levels were not altered in the Dicer1-KO livers.

It is well known that the levels of HMGCR in mammalian

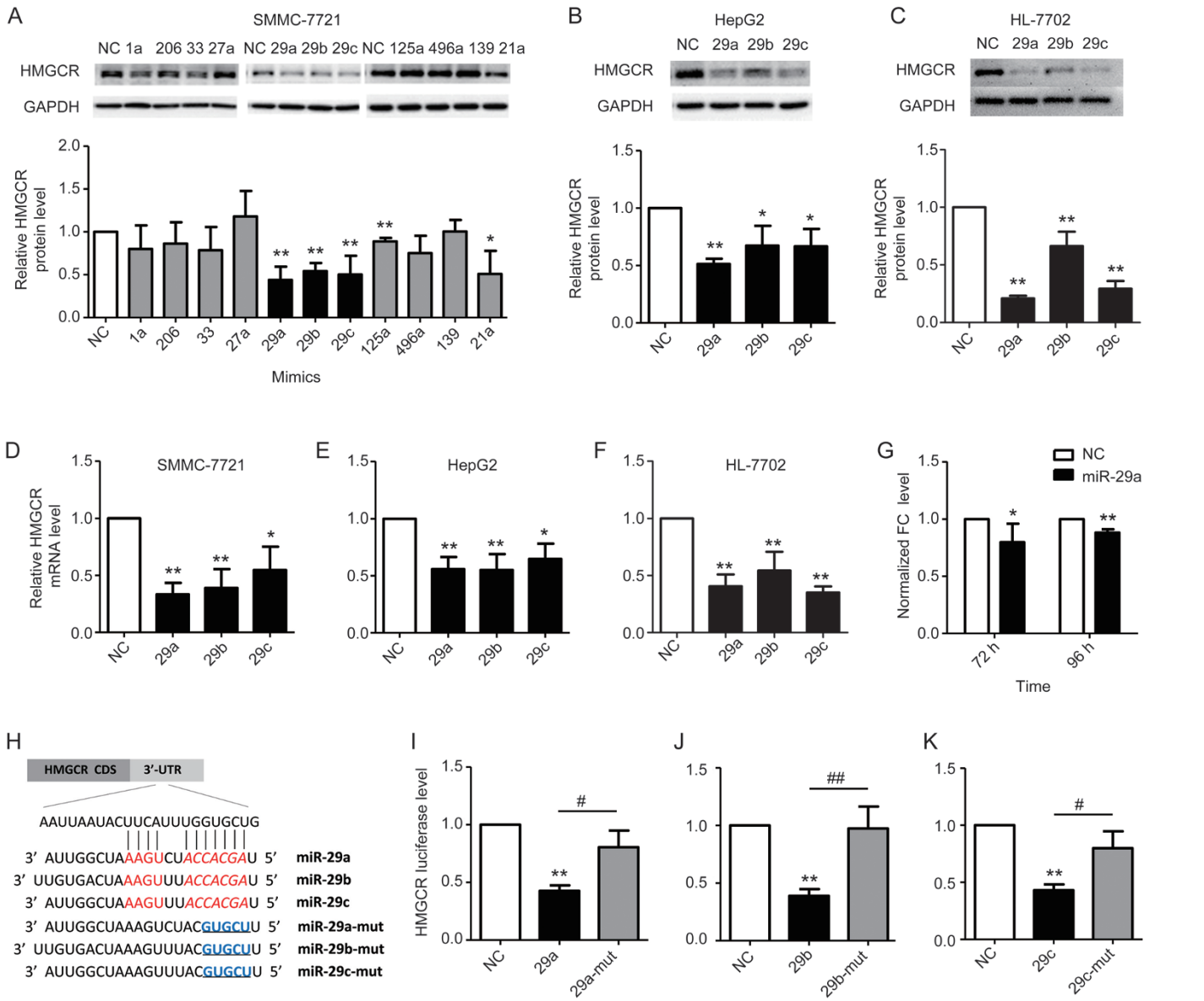

Figure 4. Overexpression of miR-29s inhibits HMGCR mRNA and protein levels by targeting HMGCR 3′-UTR, and reduces cellular free cholesterol (FC). The miRNAs which can decrease HMGCR protein expression were screened in SMMC-7721 cells (A). Overexpression of miR-29a, miR-29b and miR-29c can inhibit mRNA and protein levels of HMGCR in SMMC-7721 cells (A and D), HepG2 cells (B and E) and HL-7702 cells (C and F). FC levels were reduced after transfecting miR-29a, compared to negative control (NC) for 72 and 96 h in SMMC-7721 cells quantified by GC-MS (G). (H) Schematic of the HMGCR 3′-UTR with microRNA binding sites. Short line, predicted binding site of miRNAs at the HMGCR 3′-UTR; Italics, seed region of miRNAs; Underlined, mutations in the seed regions of miRNAs. MiR-29a (I), miR-29b (J) and miR-29c (K) reduced the luciferase activity of a luciferase reporter containing the 3′-UTR of HMGCR. Mutations (mut) in the seed regions of miR-29 reversed their inhibitory effects on luciferase activity. Data are the mean±SD of at least three independent experiments. $^{*}P<0.05$, $^{**}P<0.01$ versus negative control (NC) group. $^{\#}P<0.05$, $^{\#\#}P<0.01$ *vs* the relevant mutation.

cells are negatively regulated by cholesterol levels both transcriptionally and posttranslationally[44, 45]. However, in Dicer1-KO mouse, increased cholesterol failed to activate the negative feedback regulation of *de novo* cholesterol biosynthesis through downregulating HMGCR, which is similar to the typical characteristic of NAFLD or NASH patients[3].

Disruption of the Dicer1 gene resulted in the loss of nearly all miRNAs; therefore, alterations in the expression of their target genes and in the regulation of the cholesterol metabolism was expected. Thus, one possible explanation for the increased HMGCR expression in Dicer1-KO mouse livers may be due to some miRNAs deficiency, which prevented the targeting of HMGCR. Recent studies have shown that some miRNAs can downregulate the expression of HMGCR directly or indirectly[24, 26, 46–48]. For example, miR-21 can regulate cholesterol metabolism by targeting HMGCR directly *in vitro*[46].

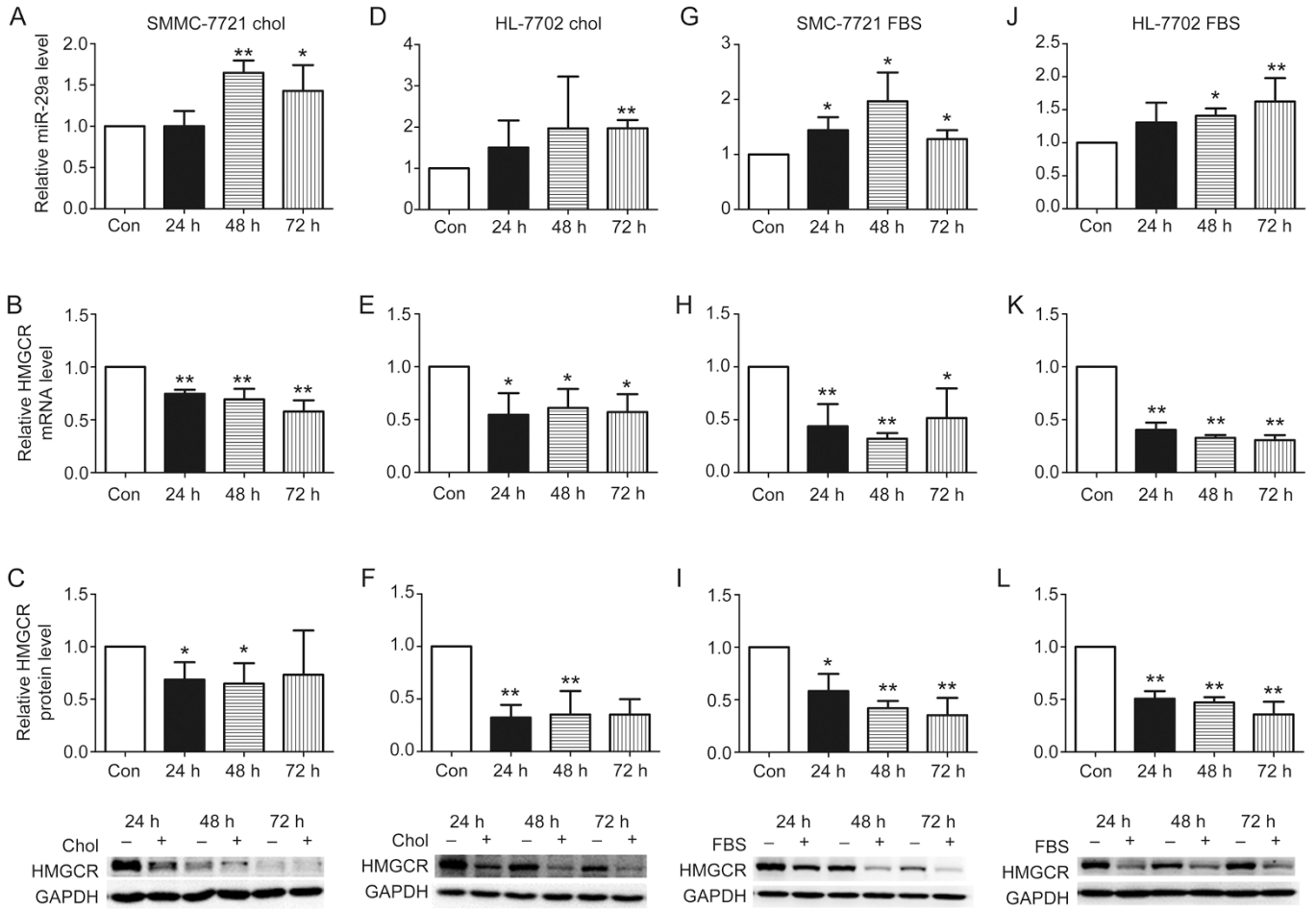

Figure 5. miR-29a levels and HMGCR levels change inversely in two steatosis hepatic cell models. (A–F) SMMC-7721 and HL-7702 cells were incubated with or without cholesterol/25-hydroxycholesterol (10 μg·mL^{-1}/1 μg·mL^{-1}) for 24 h, 48 h and 72 h. (G–L) SMMC-7721 and HL-7702 cells were exposed to 10% FBS-RPMI-1640 medium or 50% FBS-RPMI-1640 medium for 24 h, 48 h and 72 h. The miR-29a levels (A, D, G and J) and HMGCR mRNA levels (B, E, H, K) were determined by qRT-PCR, and the HMGCR protein levels (C, F, I, L) were determined by Western blot, which were normalized to control ones at the same time points. GAPDH and RNU6-2 were used as internal controls for protein and miRNA, respectively. (C and F) –, without cholesterol/25-hydroxycholesterol (chol); +, with cholesterol/25-hydroxycholesterol. (I and L) –, 10% FBS; +, 50% FBS. Data are the mean±SD of at least three independent experiments. $^{*}P<0.05$; $^{**}P<0.01$ *vs* control.

miR-185 inhibits sterol regulatory element binding protein (SREBP)-2, resulting in a decrease in cholesterol level, which reduces HMGCR expression indirectly[48].

Indeed, here, we identified miR-29a/b/c to be affected by Dicer1-deficiency; thus, their inhibitory effect on HMGCR mRNA and protein expression (Figure 4) was diminished by Dicer1 knockout. Specifically, we have revealed that miR-29a/b/c are employing their inhibitory effects by acting via their seed region to form hybrids with the 3′-UTR of HMGCR mRNA, which is in agreement with a recently published report[49].

Excess cholesterol and 25-hydroxycholesterol decreased HMGCR expression *in vitro* (Figure 5), which may be due to the increased miR-29a levels, suggesting that in normal conditions, the cells induced miR-29a expression to reduce HMGCR expression and to balance cellular cholesterol levels. However, in pathologic conditions such as NAFLD, miR-29 seemed not to be induced in the liver. A decrease of miR-29c was observed in patients with NASH versus controls[50], although the miR-29a and miR-29b levels in NAFLD need to be studied in the future. In addition, miR-29c was downregulated in NASH animal livers of C57BL/6J and DBA/2J mice fed with methyl-deficient diet, with respect to the control group[51].

Similarly, we found miR-29a was downregulated in the livers of MCD-fed mice over 3 weeks (Figure 6), and the HMGCR mRNA levels were increased, consistent with studies that found increased HMGCR expression in NASH patients[3]. An inverse correlation between miR-29a and HMGCR expression was also confirmed in the MCD diet model. Since MCD diets cause severe hepatitis, we hypothesized that the decreased hepatic miR-29a levels promoted HMGCR upregulation and FC accumulation, which in turn induced hepatocytes to develop severe steatosis and inflammation.

Mattis *et al* reported that, in the liver of mice fed with regular

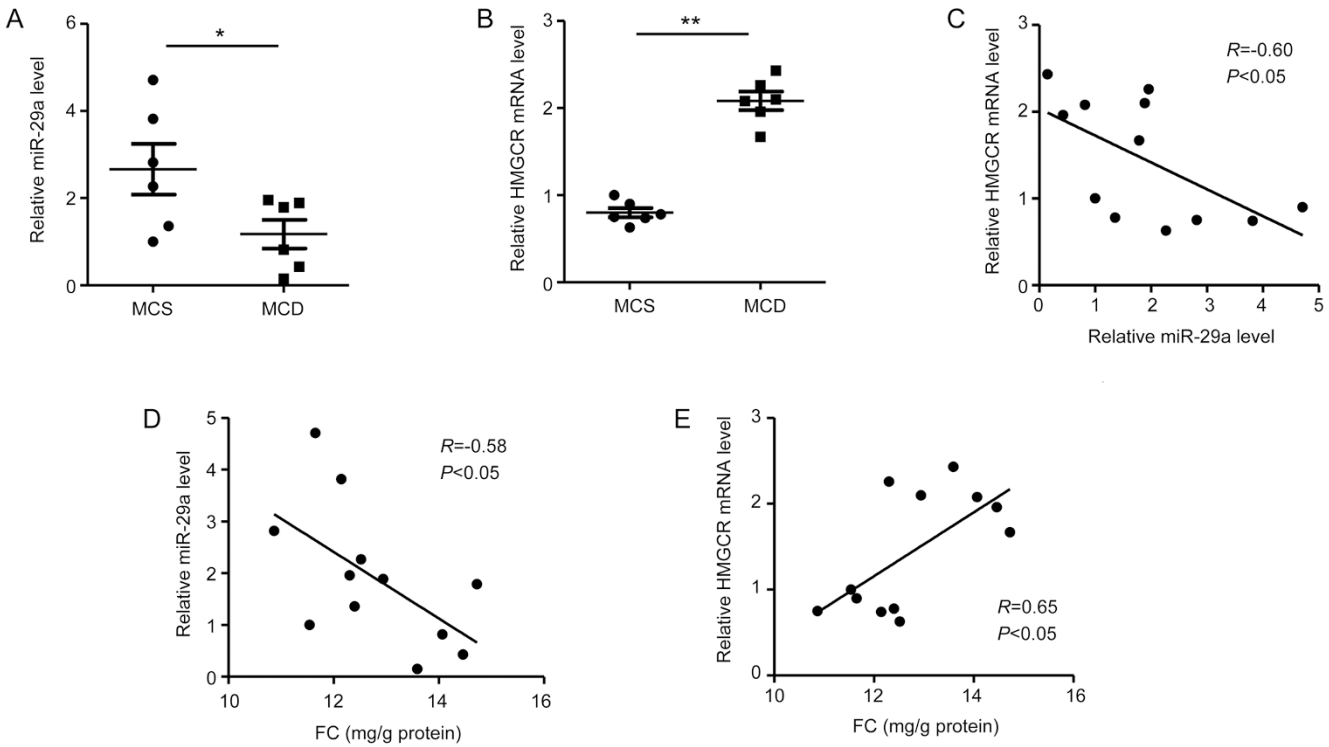

Figure 6. miR-29a levels are inversely correlated with HMGCR levels in the livers of MCD diet mouse model. C57BL/6 mice were fed either methionine-choline supplemented (MCS) control diet or methionine-choline deficient (MCD) diet for 3 weeks (n=6 for each group). The miR-29a levels (A) and HMGCR mRNA levels (B) were both determined by qRT-PCR. RNU6-2 and GAPDH were used as internal controls for miRNA and mRNA, respectively. (C) Correlation between miR-29a level and HMGCR mRNA level. (D) Correlation between free cholesterol (FC) level and miR-29a level. (E) Correlation between FC level and HMGCR mRNA level. The correlation between two variables (C, D) was determined by Pearson's correlation test. r, Pearson's correlation coefficient. mean±SEM. $^{*}P$<0.05, $^{**}P$<0.01.

chow diet, the inhibition of miR-29a resulted in marked fatty acid accumulation by targeting some fatty acid metabolism-related genes such as lipoprotein lipase. The inhibition of miR-29a also slightly increased the hepatic cholesterol level[49, 52]. However, when mice were fed with a high-fat diet (HFD) for 16 weeks, the inhibition of miR-29a caused a 2-fold FC accumulation in the liver of mice, more obvious than the accumulation of TG[52]. Combined with our results, all these lines of evidence strongly suggest that miR-29a may be a crucial regulator of hepatic cholesterol homeostasis in the progression of NAFLD. In consideration of the pivotal role of FC accumulation in NASH progression and the anti-fibrosis effect of miR-29s[53], overexpression of the miR-29 family in the liver may be a very promising therapeutic approach for NASH.

Numerous animal models of NAFLD have been reported to be used in studying the mechanisms driving the processes of NAFLD[30]. The currently available dietary models are tools to study this major human disease. The main disadvantage of the MCD model is that mice show significant weight loss and the metabolic profile of the model is opposite to that of typical human NAFLD[54]. Thus, we still currently lack a universally accepted conceptual model of NAFLD, which can completely reflect hepatic histopathology and the pathophysiology of human NAFLD. The liver-specific Dicer1-KO mouse model reflects some of the key features observed in NAFLD patients, as already described above; however, this is not fully representative of the human pathophysiology. We hope to develop further this genetic animal model and combine it with various nutritional factors in order to reflect more accurately the pathogenesis of human NAFLD in the future. Such a model would provide the means to gather valuable information for the treatment of NAFLD.

In summary, this study provides new insights into the role of Dicer1 and miRNAs in the regulation of cholesterol metabolism. The disruption of Dicer1 resulted in a marked FC and CE accumulation, which could be attributed to the observed increase of the HMGCR levels. miR-29a may decrease FC levels by regulating the expression of HMGCR. Our results, together with the known anti-fibrotic effects of miR-29a[53], suggest that miR-29a could be utilized as a potential therapeutic target for the treatment of NAFLD as well as for other liver diseases associated with FC accumulation.

Acknowledgements

The authors thank the staff at the Center for Drug Safety Evaluation and Research of Shanghai Institute of Materia Medica for their assistance with the preparation of this article.

This work was supported by grants from the National Sci-

ence and Technology Major Project [2015ZX09102005].

Author contribution

Participated in research design: Jin REN, Xin-ming QI. Conducted experiments: Ming-xia LIU, Man GAO, Chun-zhu LI, Cun-zhi YU, Hong YAN, Chun PENG, Yu LI. Performed data analysis: Ming-xia LIU, Cheng-gang LI, Ling-ling MIAO, Ze-long MA, Yang ZHAO, Meng-fan PU. Wrote or contributed to the writing of the manuscript: Jin REN, Xin-ming QI, Ming-xia LIU.

Supplementary information

Supplementary information is available on the website of Acta Pharmacologica Sinica.

References

1 Vernon G, Baranova A, Younossi ZM. Systematic review: the epidemiology and natural history of non-alcoholic fatty liver disease and non-alcoholic steatohepatitis in adults. Aliment Pharmacol Ther 2011; 34: 274–85.
2 Schuppan D, Schattenberg JM. Non-alcoholic steatohepatitis: pathogenesis and novel therapeutic approaches. J Gastroenterol Hepatol 2013; 28 Suppl 1: 68–76.
3 Min HK, Kapoor A, Fuchs M, Mirshahi F, Zhou H, Maher J, *et al*. Increased hepatic synthesis and dysregulation of cholesterol metabolism is associated with the severity of nonalcoholic fatty liver disease. Cell Metab 2012; 15: 665–74.
4 Ioannou GN. The role of cholesterol in the pathogenesis of NASH. Trends Endocrinol Metab 2016; 27: 84–95.
5 Neuschwander-Tetri BA. Hepatic lipotoxicity and the pathogenesis of nonalcoholic steatohepatitis: the central role of nontriglyceride fatty acid metabolites. Hepatology 2010; 52: 774–88.
6 Puri P, Baillie RA, Wiest MM, Mirshahi F, Choudhury J, Cheung O, *et al*. A lipidomic analysis of nonalcoholic fatty liver disease. Hepatology 2007; 46: 1081–90.
7 Tomita K, Teratani T, Suzuki T, Shimizu M, Sato H, Narimatsu K, *et al*. Free cholesterol accumulation in hepatic stellate cells: mechanism of liver fibrosis aggravation in nonalcoholic steatohepatitis in mice. Hepatology 2014; 59: 154–69.
8 Kerr TA, Davidson NO. Cholesterol and nonalcoholic fatty liver disease: renewed focus on an old villain. Hepatology 2012; 56: 1995–8.
9 Mazein A, Watterson S, Hsieh WY, Griffiths WJ, Ghazal P. A comprehensive machine-readable view of the mammalian cholesterol biosynthesis pathway. Biochem Pharmacol 2013; 86: 56–66.
10 Cohen DE, Fisher EA. Lipoprotein metabolism, dyslipidemia, and nonalcoholic fatty liver disease. Semin Liver Dis 2013; 33: 380–8.
11 Arab JP, Karpen SJ, Dawson PA, Arrese M, Trauner M. Bile acids and nonalcoholic fatty liver disease: molecular insights and therapeutic perspectives. Hepatology 2017; 65: 350–62.
12 Harfe BD, McManus MT, Mansfield JH, Hornstein E, Tabin CJ. The RNaseIII enzyme Dicer is required for morphogenesis but not patterning of the vertebrate limb. Proc Natl Acad Sci U S A 2005; 102: 10898–903.
13 Murchison EP, Partridge JF, Tam OH, Cheloufi S, Hannon GJ. Characterization of Dicer-deficient murine embryonic stem cells. Proc Natl Acad Sci U S A 2005; 102: 12135–40.
14 Kanellopoulou C, Muljo SA, Kung AL, Ganesan S, Drapkin R, Jenuwein T, *et al*. Dicer-deficient mouse embryonic stem cells are defective in differentiation and centromeric silencing. Genes Dev 2005; 19: 489–501.
15 Sekine S, Ogawa R, Ito R, Hiraoka N, McManus MT, Kanai Y, *et al*. Disruption of Dicer1 induces dysregulated fetal gene expression and promotes hepatocarcinogenesis. Gastroenterology 2009; 136: 2304–15.
16 Xie X, Miao L, Yao J, Feng C, Li C, Gao M, *et al*. Role of multiple microRNAs in the sexually dimorphic expression of Cyp2b9 in mouse liver. Drug Metab Dispos 2013; 41: 1732–7.
17 Luan Y, Qi X, Xu L, Ren J, Chen T. Absence of mature microRNAs inactivates the response of gene expression to carcinogenesis induced by *N*-ethyl-*N*-nitrosourea in mouse liver. J Appl Toxicol 2014; 34: 1409–17.
18 Jeon TI, Osborne TF. miRNA and cholesterol homeostasis. Biochim Biophys Acta 2016; 1861: 2041–6.
19 Cheung O, Puri P, Eicken C, Contos MJ, Mirshahi F, Maher JW, *et al*. Nonalcoholic steatohepatitis is associated with altered hepatic MicroRNA expression. Hepatology 2008; 48: 1810–20.
20 Salvoza NC, Klinzing DC, Gopez-Cervantes J, Baclig MO. Association of circulating serum miR-34a and miR-122 with dyslipidemia among patients with non-alcoholic fatty liver disease. PLoS One 2016; 11: e0153497.
21 Clarke PR, Hardie DG. Regulation of HMG-CoA reductase: identification of the site phosphorylated by the AMP-activated protein kinase *in vitro* and in intact rat liver. EMBO J 1990; 9: 2439–46.
22 Ono K, Horie T, Nishino T, Baba O, Kuwabara Y, Yokode M, *et al*. MicroRNA-33a/b in lipid metabolism — novel “thrifty” models. Circ J 2015; 79: 278–84.
23 Rayner KJ, Esau CC, Hussain FN, McDaniel AL, Marshall SM, van Gils JM, *et al*. Inhibition of miR-33a/b in non-human primates raises plasma HDL and lowers VLDL triglycerides. Nature 2011; 478: 404–7.
24 Goedeke L, Salerno A, Ramirez CM, Guo L, Allen RM, Yin X, *et al*. Long-term therapeutic silencing of miR-33 increases circulating triglyceride levels and hepatic lipid accumulation in mice. EMBO Mol Med 2014; 6: 1133–41.
25 Pirola CJ, Fernandez Gianotti T, Castano GO, Mallardi P, San Martino J, Mora Gonzalez Lopez Ledesma M, *et al*. Circulating microRNA signature in non-alcoholic fatty liver disease: from serum non-coding RNAs to liver histology and disease pathogenesis. Gut 2015; 64: 800–12.
26 Yamada H, Suzuki K, Ichino N, Ando Y, Sawada A, Osakabe K, *et al*. Associations between circulating microRNAs (miR-21, miR-34a, miR-122 and miR-451) and non-alcoholic fatty liver. Clin Chim Acta 2013; 424: 99–103.
27 Tsai WC, Hsu SD, Hsu CS, Lai TC, Chen SJ, Shen R, *et al*. MicroRNA-122 plays a critical role in liver homeostasis and hepatocarcinogenesis. J Clin Invest 2012; 122: 2884–97.
28 Krutzfeldt J, Rajewsky N, Braich R, Rajeev KG, Tuschl T, Manoharan M, *et al*. Silencing of microRNAs *in vivo* with 'antagomirs'. Nature 2005; 438: 685–9.
29 Hand NJ, Master ZR, Le Lay J, Friedman JR. Hepatic function is preserved in the absence of mature microRNAs. Hepatology 2009; 49: 618–26.
30 Imajo K, Yoneda M, Kessoku T, Ogawa Y, Maeda S, Sumida Y, *et al*. Rodent models of nonalcoholic fatty liver disease/nonalcoholic steatohepatitis. Int J Mol Sci 2013; 14: 21833–57.
31 Adams CM, Reitz J, De Brabander JK, Feramisco JD, Li L, Brown MS, *et al*. Cholesterol and 25-hydroxycholesterol inhibit activation of SREBPs by different mechanisms, both involving SCAP and Insigs. J Biol Chem 2004; 279: 52772–80.
32 Zhao W, Li J, He X, Lv O, Cheng Y, Liu R. *In vitro* steatosis hepatic cell model to compare the lipid-lowering effects of pomegranate peel

polyphenols with several other plant polyphenols as well as its related cholesterol efflux mechanisms. Toxicol Rep 2014; 1: 945–54.
33 Robinet P, Wang Z, Hazen SL, Smith JD. A simple and sensitive enzymatic method for cholesterol quantification in macrophages and foam cells. J Lipid Res 2010; 51: 3364–9.
34 Burg JS, Espenshade PJ. Regulation of HMG-CoA reductase in mammals and yeast. Prog Lipid Res 2011; 50: 403–10.
35 Rogers MA, Liu J, Song BL, Li BL, Chang CC, Chang TY. Acyl-CoA: cholesterol acyltransferases (ACATs/SOATs): enzymes with multiple sterols as substrates and as activators. J Steroid Biochem Mol Biol 2015; 151: 102–7.
36 Bie J, Wang J, Marqueen KE, Osborne R, Kakiyama G, Korzun W, *et al*. Liver-specific cholesteryl ester hydrolase deficiency attenuates sterol elimination in the feces and increases atherosclerosis in ldlr$^{-/-}$ mice. Arterioscler Thromb Vasc Biol 2013; 33: 1795–802.
37 Lian J, Wei E, Groenendyk J, Das SK, Hermansson M, Li L, *et al*. Ces3/TGH deficiency attenuates steatohepatitis. Sci Rep 2016; 6: 25747.
38 Go GW, Mani A. Low-density lipoprotein receptor (LDLR) family orchestrates cholesterol homeostasis. Yale J Biol Med 2012; 85: 19–28.
39 Shen WJ, Hu J, Hu Z, Kraemer FB, Azhar S. Scavenger receptor class B type I (SR-BI): a versatile receptor with multiple functions and actions. Metabolism 2014; 63: 875–86.
40 Dikkers A, de Boer JF, Groen AK, Tietge UJ. Hepatic ABCG5/G8 overexpression substantially increases biliary cholesterol secretion but does not impact *in vivo* macrophage-to-feces RCT. Atherosclerosis 2015; 243: 402–6.
41 Landgraf P, Rusu M, Sheridan R, Sewer A, Iovino N, Aravin A, *et al*. A mammalian microRNA expression atlas based on small RNA library sequencing. Cell 2007; 129: 1401–14.
42 Marí M, Caballero F, Colell A, Morales A, Caballeria J, Fernandez A, *et al*. Mitochondrial free cholesterol loading sensitizes to TNF- and Fas-mediated steatohepatitis. Cell Metab 2006; 4: 185–98.
43 Arguello G, Balboa E, Arrese M, Zanlungo S. Recent insights on the role of cholesterol in non-alcoholic fatty liver disease. Biochim Biophys Acta 2015; 1852: 1765–78.
44 DeBose-Boyd RA. Feedback regulation of cholesterol synthesis: sterol-accelerated ubiquitination and degradation of HMG CoA reductase. Cell Res 2008; 18: 609–21.
45 Song BL, Javitt NB, DeBose-Boyd RA. Insig-mediated degradation of HMG CoA reductase stimulated by lanosterol, an intermediate in the synthesis of cholesterol. Cell Metab 2005; 1: 179–89.
46 Sun C, Huang F, Liu X, Xiao X, Yang M, Hu G, *et al*. miR-21 regulates triglyceride and cholesterol metabolism in non-alcoholic fatty liver disease by targeting HMGCR. Int J Mol Med 2015; 35: 847–53.
47 Singh R, Yadav V, Kumar S, Saini N. MicroRNA-195 inhibits proliferation, invasion and metastasis in breast cancer cells by targeting FASN, HMGCR, ACACA and CYP27B1. Sci Rep 2015; 5: 17454.
48 Yang M, Liu W, Pellicane C, Sahyoun C, Joseph BK, Gallo-Ebert C, *et al*. Identification of miR-185 as a regulator of *de novo* cholesterol biosynthesis and low density lipoprotein uptake. J Lipid Res 2014; 55: 226–38.
49 Kurtz CL, Fannin EE, Toth CL, Pearson DS, Vickers KC, Sethupathy P. Inhibition of miR-29 has a significant lipid-lowering benefit through suppression of lipogenic programs in liver. Sci Rep 2015; 5: 12911.
50 Braza-Boils A, Mari-Alexandre J, Molina P, Arnau MA, Barcelo-Molina M, Domingo D, *et al*. Deregulated hepatic microRNAs underlie the association between non-alcoholic fatty liver disease and coronary artery disease. Liver Int 2016; 36: 1221–9.
51 Pogribny IP, Starlard-Davenport A, Tryndyak VP, Han T, Ross SA, Rusyn I, *et al*. Difference in expression of hepatic microRNAs miR-29c, miR-34a, miR-155, and miR-200b is associated with strain-specific susceptibility to dietary nonalcoholic steatohepatitis in mice. Lab Invest 2010; 90: 1437–46.
52 Mattis AN, Song G, Hitchner K, Kim RY, Lee AY, Sharma AD, *et al*. A screen in mice uncovers repression of lipoprotein lipase by microRNA-29a as a mechanism for lipid distribution away from the liver. Hepatology 2015; 61: 141–52.
53 Roderburg C, Urban GW, Bettermann K, Vucur M, Zimmermann H, Schmidt S, *et al*. Micro-RNA profiling reveals a role for miR-29 in human and murine liver fibrosis. Hepatology 2011; 53: 209–18.
54 Takahashi Y, Soejima Y, Fukusato T. Animal models of nonalcoholic fatty liver disease/nonalcoholic steatohepatitis. World J Gastroenterol 2012; 18: 2300–8.